

# Matched-field Source Localization with a Mobile Short Horizontal Linear Array in Offshore Shallow Water

Dexin ZHAO, Zhiping HUANG, Shaojing SU, Ting LI

*Department of Instrument Science and Technology, College of Mechatronics and Automation  
National University of Defense Technology*

47, Yanwachi Street, Changsha City, Hunan Province, 410073, P. R. China; e-mail: derekzhao27@yahoo.com

*(received July 12, 2012; accepted January 25, 2013)*

Passive source localization in shallow water has always been an important and challenging problem. Implementing scientific research, surveying, and monitoring using a short, less than ten meter long, horizontal linear array has received considerable attention in the recent years. The short array can be conveniently placed on autonomous underwater vehicles and deployed for adaptive spatial sampling. However, it is usually difficult to obtain a sufficient spatial gain for localizing long-range sources due to its limited physical size. To address this problem, a localization approach is proposed which is based on matched-field processing of the likelihood of the passive source localization in shallow water, as well as inter-position processing for the improved localization performance and the enhanced stability of the estimation process. The ability of the proposed approach is examined through the two-dimensional synthetic test cases which involves ocean environmental mismatch and position errors of the short array. The presented results illustrate the localization performance for various source locations at different signal-to-noise ratios and demonstrate the build up over time of the positional parameters of the estimated source as the short array moves at a low speed along a straight line at a certain depth.

**Keywords:** passive source localization, matched-field processing, inter-position processing, short horizontal array, shallow water.

## 1. Introduction

Passive sonar is a method for detecting acoustic signals in an underwater environment and is typically deployed in the form of long towed arrays measuring up to a thousand feet or longer to enhance the ability of detecting acoustic sources (BERNECKY, KRZYCH, 2008). The emphasis changes from detection to parameter estimation when the localization stage of sonar processing arrives (HAVELOCK *et al.*, 2008; HODGES, 2010). A number of approaches to beamforming and other acoustic source localization techniques exist. These generally include plane-wave beamforming, wavefront curvature ranging, target motion analysis, multipath ranging, and matched-field processing (MFP).

Plane-wave beamforming is the most mature of these schemes and the easiest to implement. It is assumed that the source is in the far field of the array. However, it only provides bearing information for a single linear array, and its accuracy diminishes as the source moves from the broadside to the end-fire

(HODGES, 2010; BERNECKY, KRZYCH, 2008). Wavefront curvature ranging is only accurate for near-range sources under the assumption of a spherical spread for the acoustic wavefront (HAVELOCK *et al.*, 2008).

Target motion analysis is capable of determining the source's trajectory (i.e. range, course, and speed) in the open ocean where the ray assumption is valid. It is a method that builds up the source positional parameters over time through the motion (constant velocity or maneuvering) of the source and/or the receiver. Clearly, its estimation process strongly depends on the type of measurement data and the model for the source motion and other specific problem features (HAVELOCK *et al.*, 2008; WILSON, VEENHUIS, 1997; INCE *et al.*, 2009; HODGES, 2010; BERNECKY, KRZYCH, 2008).

Multipath ranging incorporates the structure of sound propagation in the ocean into its estimation process. It is assumed that the sound radiated from a distant source arrives at the receiver via multiple paths having simple geometric interpretation (e.g. surface and bottom reflections). The process is tedious,

prone to error, and only works in specific environments (HAVELOCK *et al.*, 2008; BERNECKY, KRZYCH, 2008). It should be noted that all of the source localization techniques described thus far also do not work well in shallow water.

The shallow water environment is extremely complex, and the assumption of plane waves or other relatively simple sound propagation model in the processing scheme can lead to severe degradation of the estimation (DEBEVER, 2009; EHLERS *et al.*, 2010). As an alternative, the technique based on MFP exploits the complexity of the ocean's structure to improve source localization. Thus, the complex shallow water environment actually aids the estimation process (TOLSTOY, 1993; BAGGEROER *et al.*, 1993). This process constitutes a range-depth ambiguity surface, as it spatially correlates the actual field (measured at an array of sensors emitted from a point source at a particular location) with the replica field (computed by a numerical propagation model over a grid of hypothetical source locations). The maximum match on the ambiguity surface is regarded as the estimated source location. Given the sufficient ocean environmental information, MFP has been shown to be a promising signal processing technique. It has been used in practical applications from the stage of scientific experiments with the advent of powerful microprocessors and various optimal MFP algorithms (DEBEVER, KUPERMAN, 2007; TOLLEFSEN, DOSSO, 2009; WILSON, VEENHUIS, 1997; KIM *et al.*, 2010; FIALKOWSKI *et al.*, 1997; BERNECKY, KRZYCH, 2008).

The intent of this study is to apply MFP to a short horizontal linear array for passive source localization in a shallow water environment. The short horizontal linear array specifically refers to a passive sonar system equipped on a relatively small sensor platform, such as an autonomous underwater vehicle (MILLARD, 2003). This type of sensor platform can be conveniently deployed at any desired site in the ocean, for scientific research, surveys, and industry. It has excellent characteristics – such as low self-noise and vibration coupled with a high stability – all of which are desirable for many acoustic measurements. However, the platform also limits the array length to less than ten meters. In MFP theory, for the vertical linear array, increasing the array length to span more of the water column can significantly improve MFP sidelobe reduction and peak resolution, and the horizontal linear array usually requires a much longer array length than the vertical array for the same localization performance (TOLSTOY, 1993; TANTUM, NOLTE, 2000). The short arrays can hardly obtain sufficient spatial gain. The direct application of MFP to such arrays would result in a presumed failure in estimating the source positional parameters. The technique of synthetic aperture processing is usually used to synthesize a longer array when dealing with the problem of this

kind of mobile short horizontal linear array. The corresponding goal is to increase the bearing estimation by combing data from widely separated sampling points (AUTREY, 1988; FERNANDEZ *et al.*, 2004; WILLIAMS, HARRIS, 1992; XUDONG *et al.*, 2007). Inspired by the synthetic aperture technique, a localization approach that combines matched-field processing and inter-position processing is expected to allow for the short horizontal linear array capable of passively localizing long-range acoustic sources in range and depth rather than only bearing for the two-dimensional scenario. MFP primarily provides the likelihood of passive source localization in shallow water, and inter-position processing is used to improve the localization performance and stabilize the estimation process. Thus, the estimated source position is built up over time through combining the source localization ambiguity surfaces generated at widely separated sampling positions, as the short horizontal linear array moves at a low speed along a straight line at a certain depth.

The paper is organized as follows: Section 2 introduces the implementation of the proposed localization approach. Section 3 describes the synthetic test cases used to evaluate the capacity of the proposed approach to localize the acoustic sources in offshore shallow water. Section 4 presents and discusses the results of passive source localization using the proposed approach for various source locations at different signal-to-noise ratios (SNRs) in the presence of environmental mismatch and position errors of the short horizontal linear array. Section 5 provides a short conclusion.

## 2. Localization approach

This section describes the implementation of the proposed localization approach. In our study, the source localization ambiguity surface is generated using the incoherent broadband minimum variance (MV) processor as the short horizontal linear array moves along a straight line to each sampling position. Then, the source localization output at each sampling position is formed by averaging all of the generated ambiguity surfaces. Hence the issue of temporal and spatial coherence among the different sampling positions will not be taken into account due to an incoherent combining of the ambiguity surfaces.

In order to successfully localize the acoustic source in our problem, we have to overcome the shortcoming of the short array. We employ a high resolution MV processor to exploit as much as possible the unique information arising from the source of interest at each sampling position. The incoherent broadband processing is also used at each sampling position to increase the amount of available data and to stabilize the estimation process. It is a widely used approach to take advantage of the temporal complexity of the signal for an additional gain over narrow pro-

cessing (TOLSTOY, 1993; SOARES, JESUS, 2003; JESUS, SOARES, 2001). The inter-position processing further exploits the spatial complexity of the signal that is emitted by the source of interest and sampled by the short array as it moves to a sampling position.

The *MV* processor (also known as the minimum variance distortionless response processor and the maximum likelihood method) is a high resolution adaptive MFP method, whose essence is “optimum in the sense that the output noise power be minimized subject to the constraint of unity undistorted signal response from the desired source location” (TOLSTOY, 1993; BAGGEROER *et al.*, 1993; COX *et al.*, 1987; STRYCZNIOWICZ, 2006; LEE *et al.*, 1993). Thus, its weight vector  $w$  is determined by solving

$$\min_w \mathbf{w}^* \mathbf{R} \mathbf{w} \text{ subject to } \mathbf{w}^* \mathbf{d} = 1, \quad (1)$$

where  $\mathbf{R} = E\{\mathbf{x}\mathbf{x}^*\}$  is the cross-spectral density matrix (CSDM) at the frequency of interest,  $E\{\}$  denotes the expectation value operation, and  $\mathbf{x}$  represents the measured data vector. The superscript  $*$  denotes the conjugate transpose operation, and  $\mathbf{d}$  represents the replica vector.

The well-known solution of this optimization problem is

$$\mathbf{w}_{MV} = \frac{\mathbf{R}^{-1} \mathbf{d}}{\mathbf{d}^* \mathbf{R}^{-1} \mathbf{d}}. \quad (2)$$

The output of the *MV* processor is the square of the magnitude of the correlation between the weight vector and the measured data vector in the frequency domain, as expressed by

$$P_{MV} = \mathbf{w}_{MV}^* \mathbf{R} \mathbf{w}_{MV} = \frac{1}{\mathbf{d}^* \mathbf{R}^{-1} \mathbf{d}}. \quad (3)$$

The *MV* processor is constrained to pass the signal from the hypothetical source location (a single point on the ambiguity surface), while minimizing the response from all other locations. For high SNR cases, and in the absence of an ocean environmental mismatch, the *MV* processor ambiguity surface provides a very sharp peak where the replica vector corresponds to the data vector for the true source location, whereas it flattens the background level and suppresses sidelobes elsewhere. However, this exceptional resolution capability comes with an increased sensitivity to a slight mismatch between the modeled and actual environments. Also, the adaptive MFP methods usually require received source levels to exceed a threshold SNR (TOLSTOY, 1993; BAGGEROER *et al.*, 1993; DEL BALZO *et al.*, 1988; SMITH *et al.*, 1993; HAMSON, HEITMEYER, 1989).

Consider the noisy data vector  $\mathbf{x}_{f_j} = \mathbf{s}_{f_j} + \mathbf{n}$  received by  $N$  hydrophones in the array at the  $j$ -th frequency component. The signal vector  $\mathbf{s}_{f_j}$  and the replica vector  $\mathbf{d}_{f_j}$  are both calculated by RAM codes based on the parabolic equations (PE) theory (JENSEN *et al.*, 2011; COLLINS, 1995), and then normalized such that  $\|\mathbf{s}_{f_j}\| = 1$  and  $\|\mathbf{d}_{f_j}\| = 1$ , where  $\|\mathbf{s}_{f_j}\|$  and  $\|\mathbf{d}_{f_j}\|$

are the  $L_2$  norm of  $\mathbf{s}_{f_j}$  and  $\mathbf{d}_{f_j}$ . A common assumption is that the additive noise vector  $\mathbf{n}$  is white, Gaussian, zero-mean, and uncorrelated with the signal vector  $\mathbf{s}_{f_j}$ . Thus the components  $n_i$  in  $\mathbf{n}$  are independent random complex Gaussian variables with a zero mean. That is

$$f(n_i) = \frac{1}{\sqrt{2\pi}\sigma_n} e^{-n_i^2/2\sigma_n^2}, \quad (4)$$

where the strength of noise  $\sigma_n^2 = 1/(Nr)$ , and  $r$  denotes the input SNR averaged across the array. Since the amplitude of the signal vector varies across the array, the actual SNR on any individual hydrophone may be higher or lower. From a computational point of view, the components  $n_i$  are generated using the Box-Muller formula (PORTER, TOLSTOY, 1994):

$$n_i = \sigma_n \sqrt{-\log X_i} e^{i2\pi Y_i}, \quad (5)$$

where  $X_i$  and  $Y_i$  are random variables with a uniform distribution on the interval  $(0, 1]$ .

For each sampling position and each frequency component we generate  $L = 300$  realizations (snapshots):  $\mathbf{x}_{f_j}^l$ . The CSDM at the  $j$ -th frequency component is constructed as follows:

$$\mathbf{R}_{f_j} = E\{\mathbf{x}_{f_j} \mathbf{x}_{f_j}^*\} = \sum_{l=1}^L \mathbf{x}_{f_j}^l \mathbf{x}_{f_j}^{l*}. \quad (6)$$

Then, the normalized CSDM at the  $v$ -th sampling position is expressed by

$$\mathbf{K}_{f_j}^v = \frac{N \mathbf{R}_{f_j}^v}{(1 + \sigma_n^2)L}. \quad (7)$$

Thus, the corresponding weight vector  $\mathbf{w}_{f_j}^v$  can be calculated using Eq. (2), which yields that the source localization ambiguity surface generated by the *MV* processor at the  $j$ -th frequency component and the  $v$ -th sampling position is

$$P_{f_j}^v = \mathbf{w}_{f_j}^{v*} \mathbf{K}_{f_j}^v \mathbf{w}_{f_j}^v. \quad (8)$$

If  $M$  is the number of discrete frequencies considered, then the source localization output at the  $v$ -th sampling position is

$$P_{\text{output}} = (P_{f_1}^1 + P_{f_2}^1 + \cdots + P_{f_M}^1 + \cdots + P_{f_1}^v + P_{f_2}^v + \cdots + P_{f_M}^v) / v. \quad (9)$$

### 3. The synthetic test cases

This section introduces the synthetic test cases for evaluating the performance of the proposed localization approach. We employ a two-dimensional coordinate system, where the range  $r$  is the horizontal distance and  $z$  is the depth below the ocean surface. The test scenario is described as follows. A single static acoustic source emits multitone signals at 75 Hz, 100 Hz, 150 Hz, and 250 Hz at a fixed location. A short horizontal linear array comprised of

6 hydrophones that are evenly spaced at 1 m intervals is used to localize the source. The source is further assumed to be at the endfire of the array, and the array moves towards the source at a low speed of 2 m/s along a straight line at a 50 m depth. It should be noted that the multitone signal would arrive at the endfire of the array according to the above assumption. If the source is assumed to be at the other bearing, then the effective length of the array is shorter, and elements are more closely spaced. The relationship between the actual and effective array lengths and respective sensor positions is a function of the source range and it may be determined through trigonometric relationships (TANTUM, NOLTE, 2000). Moreover, the depth of the horizontal linear array does impact on the source localization performance attained by MFP techniques (TOLSTOY, 1993; TANTUM, NOLTE, 2000). However, this study aims to apply MFP to a short horizontal linear array for passive source localization in shallow water. In this case, we are looking forward to having a good chance of estimating the source positional parameters in depth and range rather than only bearing, as in the previous studies. The issue of examining the effects of the array depth on the localization performance is left for future research. Hence, the above test scenario assumption is justifiable.

A range-dependent ocean environmental model representative of offshore shallow water (PORTER, TOLSTOY, 1994) was chosen for this study. The model consists of a water column and a seabed with a sediment layer over a semi-infinite basement. It has a sloping bottom denoted by two parameters ( $D_1$ ) and ( $D_2$ ) as shown in Fig. 1. The seabed geoacoustic parameters include the sound speed at the top ( $c_{BD1}$ ) with respect to ( $D_1$ ) and bottom ( $c_{200}$ ) of the sediment layer, the density ( $\rho_1$ ) and attenuation ( $\alpha_1$ ) in the sediment,

and the constant sound speed equal to ( $c_{200}$ ) in the basement. The sound speed profile (SSP) in the water column is described by two parameters ( $c_0$  and  $c_{WD1}$ ) at the ocean surface and with respect to ( $D_1$ ). The sound propagation is modeled based on the PE theory (JENSEN *et al.*, 2011), in which the usual approach to the problem of simulating the basement condition is to add an artificial absorption layer of several wavelengths thickness associated with a relatively large attenuation value ( $\alpha_2 = 10$  dB/ $\lambda$ ). Table 1 shows the detailed values of the ocean environmental parameters in the simulation study.

The environmental mismatch is unavoidable and is likely the most outstanding obstacle to the general experimental application of MFP techniques. At times, the output of MFP deteriorates greatly even with low levels of the mismatch, especially for high resolution MFP methods. We use different environmental parameter sets for calculating the data vector and replica vector as shown in Table 1, thus, SSP mismatch, water depth mismatch, and mismatch in the bottom parameters are all involved in our study. Additionally, the position errors of the short horizontal linear array are introduced. In reality, we usually cannot guarantee that the positions of the array can be estimated exactly every time when the replica vectors are calculated. Hence, there always exist errors of the estimated array position in range and depth, and both are assumed to follow the uniform distribution in  $[-2$  m,  $2$  m] in our study.

We next examine the ability of the proposed approach to localize the acoustic source at three selected source locations. Source A is located at a 5.7 km range and 70 m depth, source B is located at a 6 km range and 72 m depth, and source C is located at a 8.1 km range and 58 m depth, each measured from the start

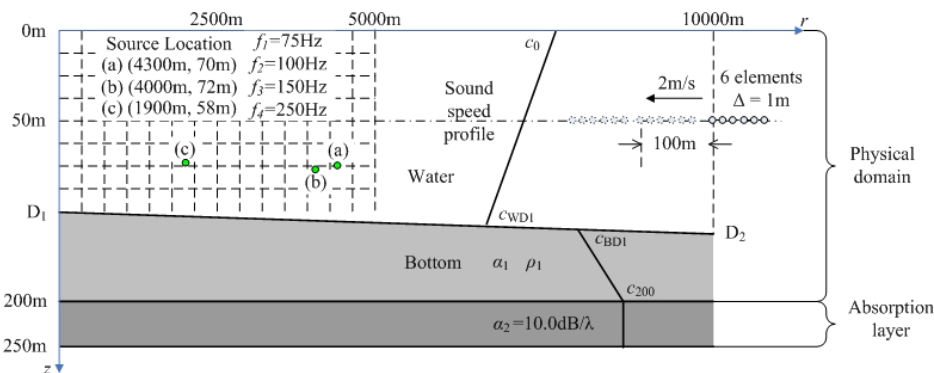


Fig. 1. Schematic of the ocean environment and the geometric configuration of the source and the array.

Table 1. Ocean environmental parameters used in the simulation study.

Parameter (unit)	$c_0$ [m/s]	$c_{WD1}$ [m/s]	$c_{BD1}$ [m/s]	$c_{200}$ [m/s]	$\alpha_1$ [dB/ $\lambda$ ]	$\rho_1$ [g/cm <sup>3</sup> ]	$D_1$ [m]	$D_2$ [m]
Data vector	1497.9	1478.3	1604	1798	0.11	1.65	101.2	104.6
Replica vector	1500	1480	1600	1750	0.35	1.75	102.5	102.5

position of the array. The estimation performance is evaluated at three SNRs, 40 dB, 10 dB, and  $-5$  dB. The search region for localizing the source extends from 0 m to 100 m in depth (spanning the entire water column), and from 5 km to 10 km in range (as measured from the start position of the array). The corresponding search grid spacing is 50 m in range and 1 m in depth. The horizontal distance between the adjacent uniformly separated sampling positions along the straight trajectory of the array is 100 m. The geometric configuration of the source and the array is also shown in Fig. 1, using relative position relationships for the source and the array based on calculation convenience.

#### 4. Results and discussion

This section presents the results of the proposed approach applied to passive source localization with a mobile short horizontal linear array. The data are simulated using the synthetic test scenarios discussed in

Sec. 3. We intend to find out how the convergence over time of the estimated source location to the true source location, and the ocean environmental mismatch and the position errors of the array affect the localization performance in our problem. To address this question, 30 sampling positions are processed. Thus, the source localization output is updated every 50 s, the interval for the updated outputs between the first and the last sampling positions is 1450 s, and the array travels up to 2.9 km until the last localization output is updated according to the above assumption. For each updated localization output, we just use the simple “peak picker” algorithm to estimate the source location with respect to the current position of the array. The localization performance in range and depth for various source locations at different SNRs is then illustrated.

Figure 2 displays the source localization outputs for source A in the high SNR case ( $\text{SNR} = 40$  dB). The six plots in this figure are selected from 30 localiza-

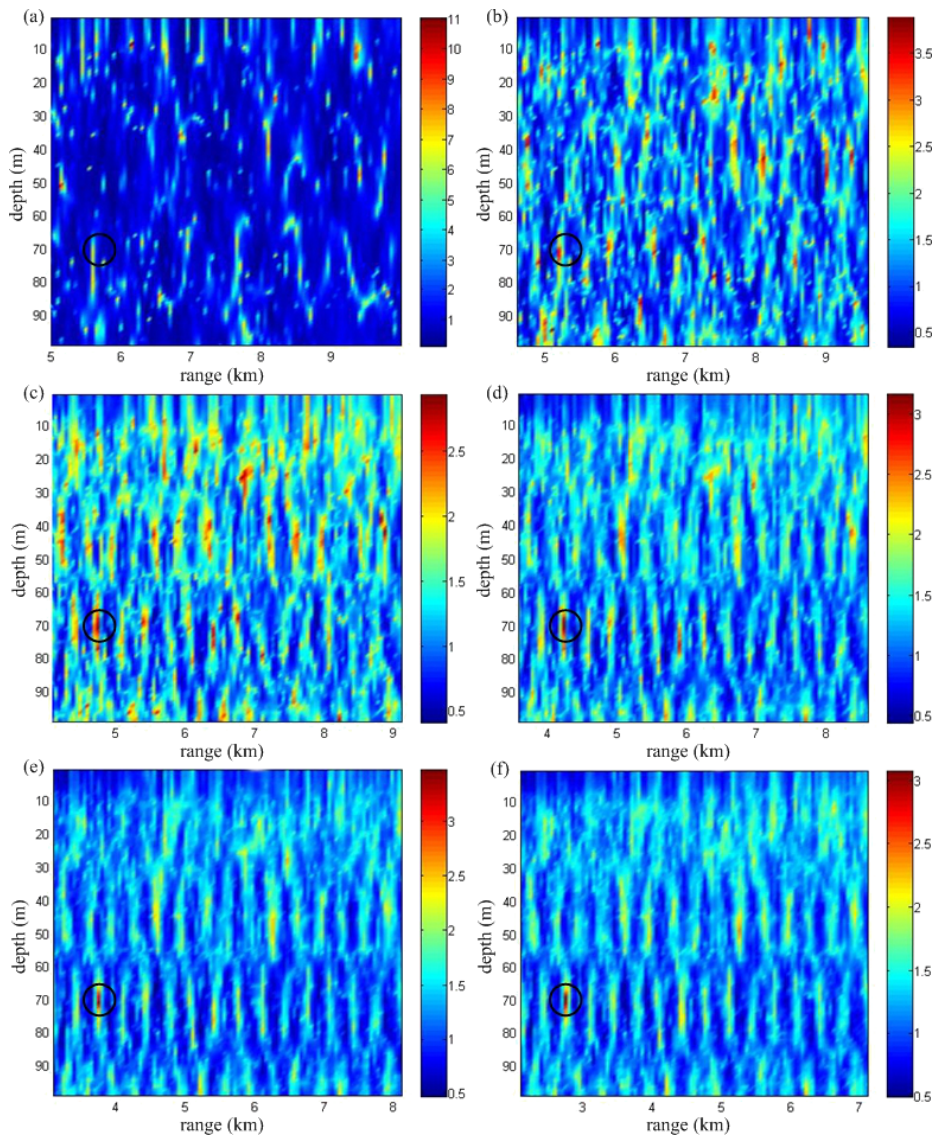


Fig. 2. Localization outputs for source A at  $\text{SNR} = 40$  dB after: a) 0 s, b) 200 s, c) 450 s, d) 700 s, e) 950 s, f) 1450 s.

Table 2. Depth and range errors of the array positions used in the simulation study.

	1	2	3	4	5	6	7	8	9	10	11	12	13	14	15
Depth error [m]	1.2	-0.8	0	0.8	1.6	2	0	-1.6	-1.6	-0.8	1.2	-0.8	1.2	-1.2	1.6
Range error [m]	-1.7	-1.8	0.1	1.1	1.7	-1.5	0.3	-0.1	-2	-0.7	-1.4	1.2	-0.8	0.1	-1.3
	16	17	18	19	20	21	22	23	24	25	26	27	28	29	30
Depth error [m]	-0.8	-1.2	-0.8	0.4	0	-0.4	1.2	0.4	0	1.6	-0.8	1.2	1.2	-0.4	0.4
Range error [m]	0.4	-0.9	0.6	0.8	1	-0.2	-1.7	-1	1.7	-1.4	1.3	0.2	2	-1.7	-0.2

tion outputs generated at 30 sampling positions. The circles denote the true source location in these plots. Figure 2 shows that the source of interest gradually appears at the correct location and that the sidelobes are better suppressed over time even in the presence of various ocean environmental mismatches and position errors of the array. Table 2 displays the depth and range errors of the array positions at each sampling position used in our simulation. It means that the incoherent broadband *MV* processor exploits the infor-

mation arising from the source of interest effectively at each sampling position at a high SNR and that its shortcoming of sensitivity to the ocean environmental mismatch and position errors of the array can be restrained through inter-position processing which not only increases the data snapshots but also exploits the spatial characteristics of the acoustic field due to the source of interest.

Figures 3 and 4 display the source localization outputs for source B at a SNR of 10 dB and source C in the

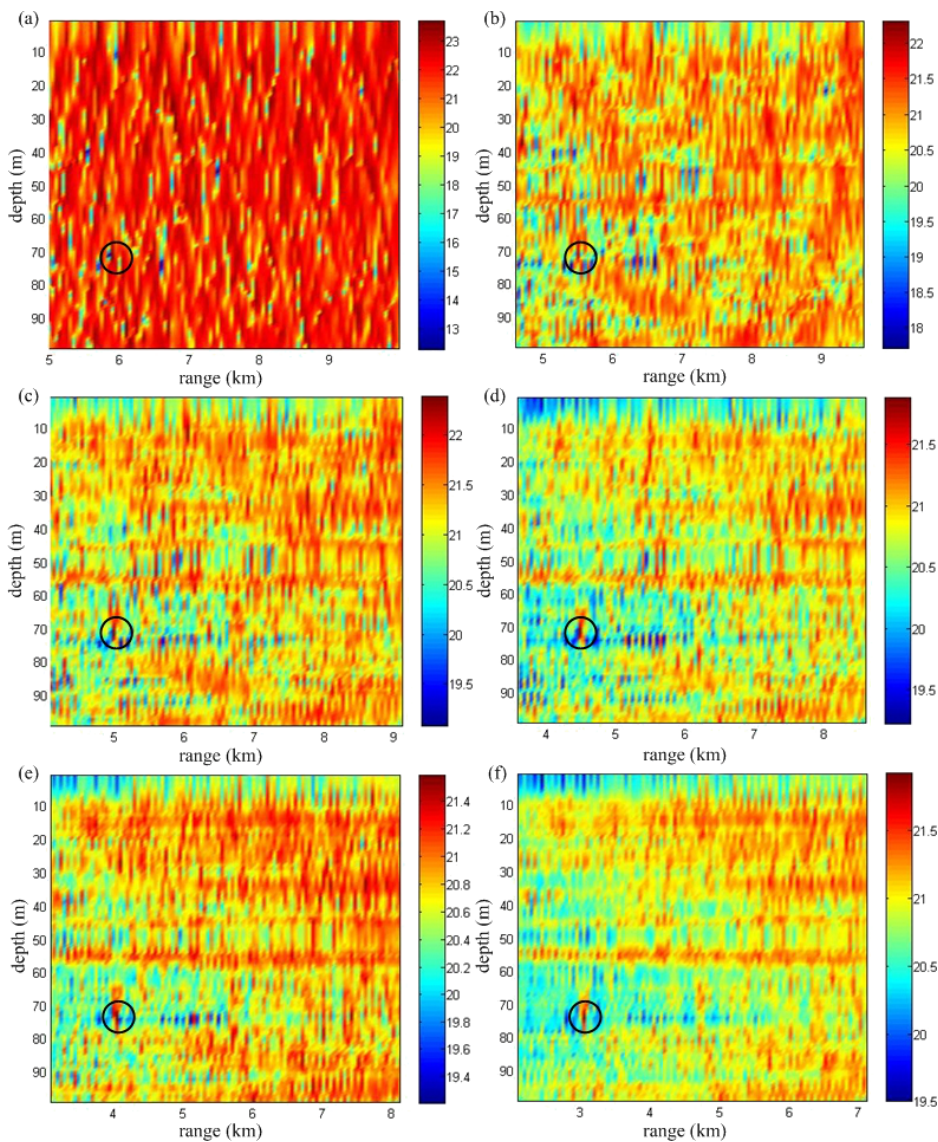


Fig. 3. Localization outputs for source B at SNR = 10 dB after: a) 0 s, b) 200 s, c) 450 s, d) 700 s, e) 950 s, f) 1450 s.

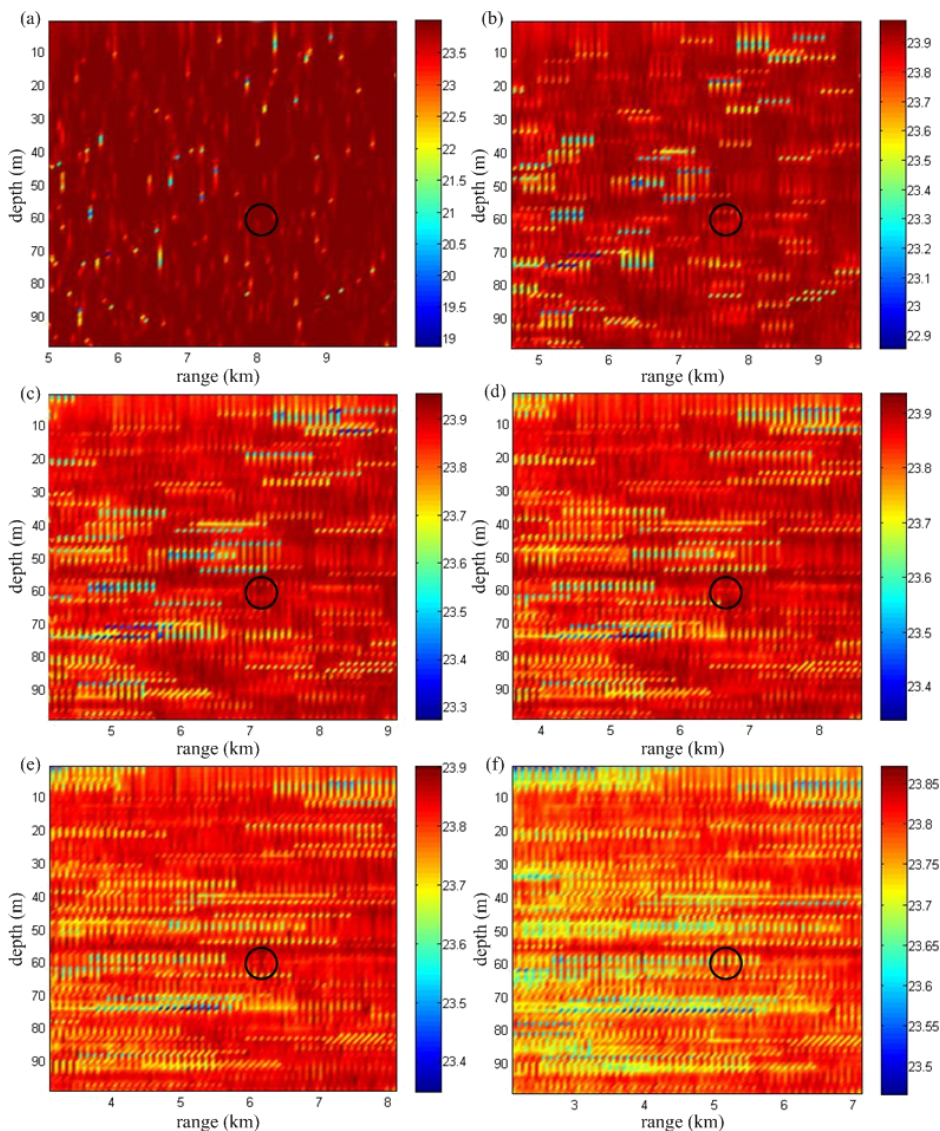


Fig. 4. Localization outputs for source C at SNR =  $-5$  dB after: a) 0 s, b) 200 s, c) 450 s, d) 700 s, e) 950 s, f) 1450 s.

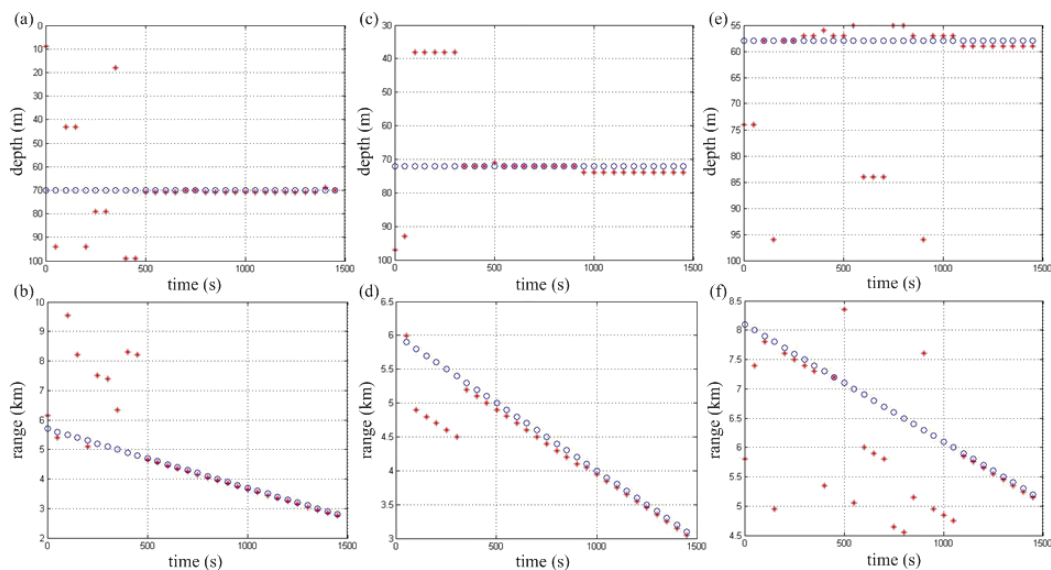


Fig. 5. a) Depth and b) range estimation *versus* time for source A at SNR = 40 dB, c) depth and d) range estimation *versus* time for source B at SNR = 10 dB, and e) depth and f) range estimation *versus* time for source C at SNR =  $-5$  dB.

case of the source of interest submerged in the white noise (SNR = -5 dB), respectively. Figure 3 shows that the source can also be localized at the correct location but with much higher sidelobes compared to the results shown in Fig. 2. However, Fig. 4 shows that the dynamic range displayed on the right side of each plot gets smaller over time and that it is already not easy to discriminate the source of interest from the background in the search region. It is seen that the localization performance degrades rapidly as the white noise level increases.

Figure 5 presents the source depth and range estimation versus the time for source A, B, and C at SNRs of 40 dB, 10 dB, and -5 dB, respectively. The circles denote the true source positional parameters, and the asterisks denote the estimated source positional parameters. The parameter estimation is considered to be acceptable if the absolute range error is less than 600m and the absolute depth error is less than 6m, as defined in (TOLLEFSEN, DOSSO, 2009). It is seen that satisfactory results are attained over time. However, the estimation process becomes extremely time-consuming when the source of interest is submerged in the noise, and the high sidelobes on the ambiguity surfaces usually make the estimated results unstable, as shown in Figs. 5e and 5f. In this case, the proposed localization approach is not realistic in practical situations. We need more resolution MFP methods to exploit more information arising from the source at each sampling position. The coherent broadband MFP that can offer additional gain (DEBEVER, KUPERMAN, 2007) may be required.

## 5. Conclusions

This paper presents an approach to passive source localization using a mobile short horizontal linear array in shallow water. The proposed approach is based on high resolution MFP methods which exploit as much as possible the information arising from the source of interest at each sampling position, as well as inter-position processing for further localization performance improvement in terms of the stability in the estimation process and the robustness to the ocean environmental mismatch and the position errors of the array. The proposed approach was applied to synthetic data in a simulated environment for three source locations at different SNRs. The results show that the source positional parameters can be built up over time, as the short horizontal linear array moves at a low speed along a straight line at a constant depth.

## Acknowledgment

This work is supported by China Shipbuilding Industry Corporation and China Scholarship Council No. 2011611091. The authors would also like to thank

Prof. Woojae Seong and Keunhwa Lee at the Underwater Acoustic Laboratory, Seoul National University, for helpful comments and discussions.

## References

1. AUTREY S. W. (1988), *Passive synthetic arrays*, Journal of the Acoustical Society of America, **84**, 592–598.
2. BAGGEROER A. B., KUPERMAN W. A., MIKHALEVSKY P. N. (1993), *An overview of matched field methods in ocean acoustics*, IEEE Journal of Oceanic Engineering, **18**, 401–424.
3. DEL BALZO D. R., FEUILLADE C., ROWE M. M. (1988), *Effects of water-depth mismatch on matched-field localization in shallow water*, Journal of the Acoustical Society of America, **83**, 2180–2185.
4. BERNECKY W. R., KRZYCH M. J. (2008), *Point source localization sonar system and method*, Patent Application Publication, United States.
5. COLLINS M. D. (1995), *User's guide for RAM versions 1.0 and 1.0p*, Naval Research Lab, Washington, DC.
6. COX H., ZESKIND R. M., OWEN M. M. (1987), *Robust adaptive beamforming*, IEEE Transactions on Acoustics, **35**, 1365–1376.
7. DEBEVER C. (2009), *Study of how environmental fluctuations influence the coherence of acoustic signals*, DTIC Document.
8. DEBEVER C., KUPERMAN W. A. (2007), *Robust matched-field processing using a coherent broadband white noise constraint processor*, Journal of the Acoustical Society of America, **122**, 1979–1986.
9. EHLERS F., FOX W., MAIWALD D., ULMKE M., WOOD G. (2010), *Advances in signal processing for maritime applications*, EURASIP Journal on Advances in Signal Processing, **2010**: 1–5.
10. FERNANDEZ J. E., MATTHEW A. D., COOK D. A., STROUD J. S. (2004), *Synthetic aperture sonar development for autonomous underwater vehicles*, OCEANS, **4**, 1927–1933.
11. FIALKOWSKI L. T., COLLINS M. D., PERKINS J. S. (1997), *Source localization in noisy and uncertain ocean environments*, Journal of the Acoustical Society of America, **101**, 3539–3545.
12. HAMSON R. M., HEITMEYER R. M. (1989), *Environmental and system effects on source localization in shallow water by the matched-field processing of a vertical array*, Journal of the Acoustical Society of America, **86**, 1950–1959.
13. MARANDA B. H. (2008), *Passive sonar*, [in:] *Handbook of signal processing in acoustics*, Havelock D., Kuwano S., Vorländer M. [Eds.], Springer, New York.
14. HODGES R. P. (2010), *Underwater acoustics: Analysis, design and performance of sonar*, Wiley, West Sussex.
15. INCE L., SEZEN B., SARIDOGAN E., INCE H. (2009), *An evolutionary computing approach for the target mo-*



- tion analysis (TMA) problem for underwater tracks, *Expert Systems with Applications*, **36**, 3866–3879.
16. JENSEN F. B., KUPERMAN W. A., PORTER M. B., SCHMIDT H. (2011), *Computational ocean acoustics*, Springer, New York.
  17. JESUS S. M., SOARES C. (2001), *Broadband MFP: coherent vs. incoherent*, *OCEANS*, **2**, 776–781.
  18. KIM K., SEONG W., LEE K. (2010), *Adaptive surface interference suppression for matched-mode source localization*, *IEEE Journal of Oceanic Engineering*; **35**, 120–130.
  19. LEE Y. P., MIKHALEVSKY P., FREESE H., HANNA J. (1993), *Robust adaptive matched-field processing*, *OCEANS*, **3**, 387–392.
  20. MILLARD N. W. (2003), *Multidisciplinary ocean science applications of an AUV: the autosub science missions programme*, [in:] *Technology and Applications of Autonomous Underwater Vehicles*, Griffiths G. [Ed.], Taylor & Francis, London and New York.
  21. PORTER M. B., TOLSTOY A. (1994), *The matched-field processing benchmark problems*, *Journal of the Acoustical Society of America*, **2**, 161–185.
  22. SMITH G. B., CHANDLER H. A., FEUILLADE C. (1993), *Performance stability of high-resolution matched-field processors to sound-speed mismatch in a shallow-water environment*, *Journal of the Acoustical Society of America*, **93**, 2617–2626.
  23. SOARES C., JESUS S. M. (2003), *Broadband matched-field processing: coherent and incoherent approaches*, *Journal of the Acoustical Society of America*, **113**, 2587–2598.
  24. STRYCZNIEWICZ L. (2006), *The methods of inversion and the maximum likelihood estimation in acoustic tests of industrial sources in the environment*, *Archives of Acoustics*, **31**, 4S, 295–301.
  25. TANTUM S. L., NOLTE L. W. (2000), *On array design for matched-field processing*, *Journal of the Acoustical Society of America*, **107**, 2101–2111.
  26. TOLLEFSEN D., DOSSO S.E. (2009), *Three-dimensional source tracking in an uncertain environment*, *Journal of the Acoustical Society of America*, **125**, 2909–2917.
  27. TOLSTOY A. (1993), *Matched field processing for underwater acoustics*, World Scientific, Singapore.
  28. WILLIAMS R., HARRIS B. (1992), *Passive acoustic synthetic aperture processing techniques*, *IEEE Journal of Oceanic Engineering*, **17**, 8–15.
  29. WILSON J. H., VEENHUIS R. S. (1997), *Shallow water beamforming with small aperture, horizontal, towed arrays*, *Journal of the Acoustical Society of America*, **101**, 384–394.
  30. XUDONG Y., JIANGUO H., QUNFEI Z., QI T. (2007), *Study on the long-distance target apperception techniques for underwater vehicles*, *Journal of Systems Engineering and Electronics*, **18**, 484–490.